EUROPEAN ORGANIZATION FOR NUCLEAR RESEARCH
CERN - SPS DIVISION

CERN SPS/85-36 (DI-MST)

Hamiltonian Analysis of Synchro-Betatron Resonances due to a Crossing Angle

Yong Ho Chin

Prévessin - 5th August 1985

CONTENTS

I. Introduction

When two bunches pass through one another with a crossing angle at the collision point, the transverse kick which a particle receives due to the space charge force produced by the incoming bunch is a function of not only its transverse position but also its longitudinal position. The longitudinal momentum is also changed by the amount given by the projection of this kick into the longitudinal coordinate. This mechanism which couples the betatron and the synchrotron motions excites a synchro-betatron resonance when the betatron tune ν_x and the synchrotron tune ν_s satisfy the condition:

$$p\nu_x + q\nu_s \tilde{=} n \quad ,$$

where p, q, and n are integers. This effect has limited the luminosity of the storage ring DORIS[1].

The synchro-betatron resonances including ones driven by other mechanisms were investigated quite thoroughly by Piwinski[1] using both analytical methods[2] and computer simulations[3]. Some of the main characteristics of the resonance effects were derived by him from the Hamiltonian[2], and agree with the results of computer simulations. However, since the final form of the Hamiltonian is hard to calculate numerically, the dynamics of particle motion was studied only by tracking particle trajectories.

The computer simulations for DORIS[3] show that in spite of a relatively small tune shift parameters $\xi = 0.01$, betatron motion can reach an amplitude more than 50% larger than the initial value, and particle trajectories look quite periodic. The width of most resonances is very small ($\lesssim 0.001$) compared to the spacing between resonances. These observations imply that the essential nature of the synchro-betatron resonance is not governed by chaotic behaviour due to e.g. resonance overlap, but is just due to single resonance effects.

Remembering this, we will analyse the synchro-betatron resonance due to a crossing angle using the Hamiltonian and the single resonance model. Since the other transverse plane which does not have a crossing angle plays no important role in the matter, we restrict our problem to the two-dimensional system. In addition, we limit our treatment of the beam-beam interaction to the "strong-weak" case, namely, only the particles in the weak beam are perturbed by the beam-beam force.

The plan of the paper is as follows. In Sec. II, by the canonical transformations and some painful algebra, we will derive the Hamiltonian in a form computable easily and quickly. We pick up a single resonance from the Hamiltonian in Sec. III, assuming that the tune is very close to that resonance. Some characteristics of the resonance effect derived by Piwinski are rederived there. We will find a constant of motion at this stage, thus reducing the problem to one-dimension. The statics and the dynamics of particle motion are discussed in Sec. IV and V. The theory is compared to computer simulations for the DORIS. In Sec. VI, we try some qualitative discussions about the equilibrium particle distribution eventually obtained in the presence of the resonance, but the radiation damping and the quantum excitation are not included, so that treatment is limited to a proton beam. We conclude the work in Sec. VII.

II. Hamiltonian

The starting point is the well-known Hamiltonian[4)]

$$H = \frac{1}{2} p_x^2 + \frac{1}{2} Kx^2 - \frac{\eta \omega_{rf}^2}{2c^2\beta^2} W^2 - \frac{eV}{2\pi\omega_{rf} p_0 R} (\cos(\Phi_s + \Delta\Phi) + (\Phi_s + \Delta\Phi)\sin\Phi_s) + U(x + \frac{aR}{h}\Delta\Phi) \sum_{n=-\infty}^{\infty} \delta(s - 2\pi Rn), \qquad (2.1)$$

where $U(x + \frac{aR}{h}\Delta\Phi)$ is the potential of beam-beam force at a crossing angle 2a. The successive collisions are expressed by an infinite series of δ-functions. For simplicity only one collision per

revolution is assumed. Here x is the transverse coordinate which has a crossing angle, and p_x is the canonical momentum conjugate to x. The other transverse coordinate which does not have a crossing angle, and hence does not contribute to the synchro-betatron resonance, is ignored.

The symbol $\Delta\Phi$ representing the synchrotron coordinate is the rf phase angle relative to the synchronous phase Φ_s. We have $W = -\frac{\Delta E}{p_o \omega_{rf}}$ as the canonical momentum conjugate to $\Delta\Phi$ where ΔE is the energy deviation from the centre energy. All the other notations are as follows:

K	=	$\frac{1}{\rho^2} + \frac{1}{B\rho}\frac{\partial B}{\partial x}$
ρ	=	radius of curvature
B	=	magnetic induction
η	=	$\alpha - \frac{1}{\gamma^2}$
α	=	momentum compaction factor
$\beta.\gamma$	=	Lorentz factor
c	=	speed of light
h	=	harmonic number
ω_{rf}	=	$h\omega_o$ = rf angular frequency
ω_o	=	angular revolution frequency
e	=	elementary charge
V	=	rf voltage
p_o	=	central momentum
R	=	average radius.

The form of U depends on the particle distribution of the strong beam. Assuming a Gaussian distribution, U is written as [2)]

$$U(z) = 8\pi\xi \frac{\sigma^2}{\beta_x^*} \int_o^z \frac{1}{u}\left(1 - e^{-\frac{u^2}{2\sigma^2}}\right) du \quad , \qquad (2.2)$$

where ξ is the beam-beam parameter, β_x^* is the beta-function at the collision point, and σ is the effective standard deviation of the transverse bunch size given by

$$\sigma = \sqrt{\sigma_x^2 + a^2\sigma_s^2} \quad , \tag{2.3}$$

where σ_x and σ_s are the standard deviations of beam size in the collision point for the transverse and longitudinal direction, respectively.

We change the independent variable from s to the angular position θ defined by

$$\theta = \frac{s}{R} \quad , \tag{2.4}$$

and the Hamiltonian is multiplied by R. The summation of δ-functions can be Fourier expanded using the property $\delta(ax) = \frac{1}{|a|}\delta(x)$ and Poisson's formula;

$$\sum_{n=-\infty}^{\infty} \delta(s - 2\pi Rn) = \frac{1}{2\pi R} \sum_{k=-\infty}^{\infty} e^{-i2\pi k\theta} \quad . \tag{2.5}$$

Now, we transform to action-angle variables (Ψ_x, I_x, Ψ_s, I_s) through a canonical transformation using the generating function

$$G = \frac{c\beta\nu_s}{2h^2|\eta|\omega_0} (\Delta\Phi)^2 \tan \Psi_s - \frac{x^2}{2\beta_x} \tan (W_x + \Psi_x) + \frac{\beta_x'}{\beta_x} x^2 \tag{2.6}$$

with

$$W_x = \int_0^s \frac{ds}{\beta_x} - \nu_x\theta \quad . \tag{2.7}$$

The old and the new coordinates are related by

$$x = (2\beta_x I_x)^{1/2} \cos(W_x + \Psi_x) \quad , \tag{2.8}$$

$$p_x = -\left(\frac{2I_x}{\beta_x}\right)^{1/2}[\alpha_x \cos(W_x + \Psi_x) + \sin(W_x + \Psi_x)] \quad , \tag{2.9}$$

$$\Delta\Phi = \left(\frac{2h^2|\eta|\omega_o}{c\beta\nu_s} I_s\right)^{1/2} \cos\Psi_s \quad , \tag{2.10}$$

$$W = -\left(\frac{2c\beta\nu_s}{h^2|\eta|\omega_o} I_s\right)^{1/2} \sin\Psi_s \quad . \tag{2.11}$$

The new Hamiltonian is

$$H = \nu_x I_x - \nu_s I_s + H_1 \tag{2.12}$$

with

$$H_1 = U((2\beta_x^* I_x)^{1/2} \cos(W_x + \Psi_x) + a\left(\frac{2|\eta|R}{\beta\nu_s} I_s\right)^{1/2} \cos\Psi_s) \bullet \frac{1}{2\pi} \sum_{k=-\infty}^{\infty} e^{-i2\pi k\Theta} \quad . \tag{2.13}$$

The case above transition energy is assumed here.

The potential U is difficult to handle as it is in the integral form. In order to work out the integration, we expand the exponential in polynomials, putting off the problem of slow convergence. We obtain

$$U = \frac{8\pi\xi\sigma^2}{\beta_x^*} \sum_{n=1}^{\infty} \frac{(-1)^{n+1}}{n!\ 2n} (\alpha_x \cos(W_x + \Psi_x) + \alpha_s \cos\Psi_s)^{2n}, \tag{2.14}$$

where we used the abbreviation

$$\alpha_x = \frac{1}{\sqrt{2\sigma}} (2\beta_x^* I_x)^{1/2} \tag{2.15}$$

and

$$\alpha_s = \frac{a}{\sqrt{2\sigma}} \left(\frac{2|\eta|R}{\beta\nu_s} I_s\right)^{1/2} \quad . \tag{2.16}$$

Furthermore we expand each term $(\alpha_x \cos(W_x + \Psi_x) + \alpha_s \cos\Psi_s)^{2n}$ into a normal binomial series, when we notice that we can rearrange the whole series as follows (see Appendix A-1):

$$U = \frac{8\pi\xi\sigma^2}{\beta_x^*} \Big[\sum_{m=o}^{\infty} \sum_{\ell=o}^{\infty} a_{\ell+m}\, 2(\ell+m)\, C_{2\ell} (\alpha_x \cos(W_x + \Psi_x))^{2m} (\alpha_s \cos\Psi_s)^{2\ell}$$

$$+ \sum_{m=1}^{\infty} \sum_{\ell=1}^{\infty} a_{\ell+m-1}\, 2(\ell+m-1)\, C_{2\ell-1} (\alpha_x \cos(W_x + \Psi_x))^{2m-1} (\alpha_s \cos\Psi_s)^{2\ell-1} \Big] , \tag{2.17}$$

where ${}^nC_m$ is the binomial coefficient:

$${}^nC_m = \frac{n!}{(n-m)!\, m!} \tag{2.18}$$

and

$$a_n = \frac{(-1)^{n+1}}{n!\, 2n} \qquad (n \geq 1)$$

$$= 0 \qquad (n = o) \quad . \tag{2.19}$$

The multipoles of the cosine-function are also expanded using the formulae

$$\cos^{2n}\theta = \frac{1}{2^{2n-1}} \Big[\sum_{r=o}^{n-1} {}^{2n}C_r \cos(2n-2r)\theta + \frac{1}{2}\, {}^{2n}C_n \Big) \quad , \tag{2.20}$$

$$\cos^{2n-1}\theta = \frac{1}{2^{2n}} \bullet \sum_{r=o}^{n} {}^{2n+1}C_r \cos(2n-2r+1)\theta \quad . \tag{2.21}$$

If we rearrange the resulting quadrupole summation in order of the resonances, after painful algebra (see Appendix A.2) we finally get

$$U = \frac{2\pi\xi\sigma^2}{\beta_x^*}\left[F_{oo}(\alpha_x, \alpha_s) + \sum_{-\infty<p,\ q<\infty}{}' F_{pq}(\alpha_x,\alpha_s)\cos(p(W_x + \Psi_x) + q\Psi_s)\right] , \tag{2.22}$$

where

$$F_{pq} = \alpha_x^{|p|}\alpha_s^{|q|}\sum_{m=o}^{\infty}\sum_{\ell=o}^{\infty} b_{m+\ell+\frac{|p|+|q|}{2}} \frac{\alpha_x^{2m}\ \alpha_s^{2\ell}}{m!\ (m+|p|)!\ \ell!(\ell+|q|)!} \tag{2.23}$$

with

$$b_n = \frac{(-1)^{n+1}(2n!)}{n \cdot n!\ 2^{2n-1}} (n \geq 1)$$

$$= 0 \qquad\qquad (n = o) . \tag{2.24}$$

The prime in the summation mark means that p = q = o term is excluded from the summation and p + q must be even. The second constraint on the combination of p and q follows from the symmetry of the potential[2)]

$$U(z) = U(-z) . \tag{2.25}$$

This can easily be seen by looking at the structure of Eq. (2.17) where no polynomial is multiplied by the polynomial of different polarity of the other coordinate.

By combining the cosine terms with the Fourier series in Θ in Eq. (2.13), the perturbation Hamiltonian can be written as

$$H_1 = \xi\frac{\sigma^2}{\beta_x^*}\left[F_{oo}(\alpha_x, \alpha_s) + \sum_{-\infty<p,q,k<\infty}{}' F_{pq}(\alpha_x, \alpha_s)\cos(p(W_x + \Psi_x) + q\Psi_s - k\Theta)\right] . \tag{2.26}$$

It should be pointed out that the Hamiltonians so far are all "time (Θ here)" – dependent because of the explicit Θ dependence.

III. Single resonance

Now, suppose that the tune ν_x and ν_s are very close to the values which satisfy $p\bar{\nu}_x - q\bar{\nu}_s = k$, we pick up only the slowly varying term, and drop all other fast-oscillating terms which even out over a few turns. This can be done by moving to coordinates which rotate in each phase space with the tune $\bar{\nu}_x$ and $\bar{\nu}_s$ by applying a canonical transformation whose generating function is

$$G = \tilde{I}_x(\Psi_x + W_x - \bar{\nu}_x\theta) + \tilde{I}_s(\Psi_s + \bar{\nu}_s\theta) \quad . \tag{3.1}$$

The new set of action-angle variables are:

$$\tilde{I}_x = I_x \quad , \tag{3.2}$$

$$\bar{\Psi}_x = \Psi_x + W_x - \bar{\nu}_x\theta \quad , \tag{3.3}$$

$$\tilde{I}_s = I_s \quad , \tag{3.4}$$

$$\bar{\Psi}_s = \Psi_s + \bar{\nu}_s\theta \quad . \tag{3.5}$$

The Hamiltonian becomes

$$H_r = \delta_x I_x - \delta_s I_s + H_1 , \tag{3.6}$$

where

$$H_1 = \frac{\xi\sigma^2}{\beta_x^*}\left[F_{oo}(\alpha_x,\alpha_s) + 2\cos(p\bar{\Psi}_x + q\bar{\Psi}_s)\, F_{pq}(\alpha_x,\alpha_s)\right] \quad , \tag{3.7}$$

and

$$\delta_\alpha = \nu_\alpha - \bar{\nu}_\alpha \quad (\alpha = x, \text{ or } s) \quad .$$

This Hamiltonian is now a constant of motion, that is, there is no explicit time-dependence. If we can find another constant of motion, the problem is solved in the sense that the particle motion is completely predictable with those two constants of motion as parameters[5]. Such a system is called integrable mathematically. In fact, the second constant of motion is found already by Piwinski[2]. If we calculate Hamilton's equations for I_x and I_s, it turns out that the following combination of I_x and I_s is conserved.

$$\frac{d}{d\theta}\,(-\,qI_x + pI_s) = 0 \quad . \tag{3.8}$$

We define this constant of motion by

$$C = -\,qI_x + pI_s \quad . \tag{3.9}$$

The problem is now no longer two-dimensional, but only one-dimensional. The new single set of variable coordinates is the coupled variable

$$J = pI_s + qI_x \quad , \tag{3.10}$$

and the slow phase

$$\Psi = \frac{p\bar{\Psi}_x + q\bar{\Psi}_s}{2pq} \quad . \tag{3.11}$$

The canonical transformation with the generating function[6]

$$G = [J(p\bar{\Psi}_x + q\bar{\Psi}_s) - C(p\bar{\Psi}_x - q\bar{\Psi}_s)]/2pq \tag{3.12}$$

yields the one-dimensional Hamiltonian

$$H_c = J\delta_- - C\delta_+ + \xi\,\frac{\sigma^2}{\beta^*_x}\,[F_{oo}(J,C) + 2\cos(2pq\Psi)F_{pq}(J,C)] \quad , \tag{3.13}$$

where

$$\delta_{\pm} = \frac{1}{2} \left(\frac{\delta_x}{q} \pm \frac{\delta_s}{p} \right) . \qquad (3.14)$$

The canonical angle Ψ_c conjugate to C which does not appear in the Hamiltonian is

$$\Psi_c = - \frac{p\bar{\Psi}_x - q\bar{\Psi}_s}{2pq} . \qquad (3.15)$$

Before going to the dynamics problem, let us repeat the remark pointed out by Piwinski on the sum and the difference resonances[1]. In the $(\bar{\nu}_x, \bar{\nu}_s)$ tune diagram, the lines of difference resonances run diagonally with positive slope, while in the normal difference resonances occurring between the two transverse oscillations, those lines run with negative slope. Therefore when the "difference" of the tunes becomes integer, the "difference resonance" is excited. This is simply due to the fact that the direction of synchrotron oscillation is contrary to the betatron oscillation above the transition energy. The minus sign in front of ν_s in Eq. (2.12) appears for this reason.

IV. Statics

We introduce some functions[7] and fixed points in the phase space from the Hamiltonian H_c of (3.13). The equations of motion are given by

$$\frac{dJ}{d\theta} = - \frac{\partial H_c}{\partial \Psi} = 4pq\xi \frac{\sigma^2}{\beta_x^*} \sin (2pq\Psi) F_{pq}(J,C) , \qquad (4.1)$$

$$\frac{d\Psi}{d\theta} = \frac{\partial H_c}{\partial J} = \delta_- + \xi \frac{\sigma^2}{\beta_x^*} \left[\frac{\partial F_{oo}}{\partial J} + 2\cos(2pq\Psi) \frac{\partial F_{pq}}{\partial J} \right] . \qquad (4.2)$$

The second term in Eq. (4.2) defines the nonlinear detuning term

$$\nu_{NL}(J,C) = \xi \frac{\sigma^2}{\beta^*_x} \frac{\partial F_{oo}}{\partial J} \tag{4.3}$$

which gives the change of tune with amplitude J, and is the same for all the resonances. At zero amplitude, the tune shift is ξ, and then monotonously decreases to zero as the amplitude increases. The third term in Eq. (4.2) gives the resonance width in tune units:

$$\nu_{pq}(J,C) = 2\ \xi \frac{\sigma^2}{\beta^*_x} \frac{\partial F_{pq}}{\partial J} \quad . \tag{4.4}$$

Thus, the effective tune of a particle with a certain amplitude J is within $\pm\ \nu_{pq}(J,C)$ around $\delta_- + \nu_{NL}(J,C)$.

The fixed points of motion are obtained by the conditions

$$\frac{dJ}{d\theta} = \frac{d\Psi}{d\theta} = 0 \tag{4.5}$$

which lead to

$$\sin\ (2pq\Psi) = 0 \tag{4.6}$$

and

$$\delta_- + \nu_{NL}(J,C) + \cos(2pq\Psi)\nu_{pq}(J,C) = 0 \ . \tag{4.7}$$

Of the solutions for Eqs. (4.6) and (4.7),

$$\cos(2pq\Psi) = (-1)^{\frac{|p| + |q|}{2}}$$

gives the unstable fixed point J_u, while

$$\cos(2pq\Psi) = (-1)^{\frac{|p| + |q|}{2} + 1}$$

gives the stable fixed point J_s.

A few comments can be made on these quantities using practical machine parameters of the DORIS which are listed in Table I. They are the same as used by Piwinski[3]. The nonlinear detuning term can be calculated from the partial derivatives of F_{oo} with respect to α_x and α_s:

$$\nu_{NL}(J,C) = \xi \frac{\sigma^2}{\beta^*_x} \left[\frac{\partial \alpha_x}{\partial J} \frac{\partial F_{oo}}{\partial \alpha_x} + \frac{\partial \alpha_s}{\partial J} \frac{\partial F_{oo}}{\partial \alpha_s} \right]_{C = \text{const}}$$

$$= \xi \left[\frac{1}{2q} \sum_{s=o}^{\infty} \sum_{m=1}^{\infty} \frac{b_{m+s}^{m}}{s!^2\, m!^2} \alpha_s^{2s} \alpha_x^{2(m-1)} \right.$$

$$\left. + \frac{a^2 |\eta| R}{\beta \nu_s} \cdot \frac{1}{2p} \sum_{s=1}^{\infty} \sum_{m=0}^{\infty} \frac{b_{m+s}^{s}}{s!^2\, m!^2} \alpha_s^{2(s-1)} \alpha_x^{2m} \right] . \qquad (4.8)$$

The factor $a^2 |\eta| R/\beta\nu_s$ for DORIS is about 1/300, and therefore the second term is negligibly small compared to the first term. The solid line in Fig. 1 shows the detuning curve in units of ξ, while the broken line shows the contribution of the second term to it, from which the statement above can be confirmed. Attention should be paid to the point that the detuning function starts from the value slightly less than 1, since there is detuning due to non-zero synchrotron amplitude.

The order of magnitude of I_x is usually much smaller than that of I_s : $I_x/I_s \sim 10^{-2}$ for the DORIS parameters. Doubling the transverse beam size causes only 2% change in the synchrotron amplitude. The situation is similar to the flat-beam case[8,9] where the vertical emittance is an order of magnitude smaller than the horizontal one, however, the ratio is still an order of magnitude bigger than the present case. Speaking from the view of analogy with thermodynamics, the transverse motion can be said to be in the system which is in "thermal contact" with the isothermal system of

synchrotron motion, and can absorb the energy from these without perturbing it. The synchrotron amplitude is kept almost constant in the dynamic motion, and thus practically, giving a constant of motion C makes the same sense as fixing a synchrotron amplitude.

From the arguments mentioned above, we can demonstrate what follows on the sum and the difference resonances which have the same combination of p,q and k, but different sign of q. First, since the second term in Eq. (4.8) is negligible, the amount of detuning for the sum resonance is as big as for the difference resonance. In the flat-beam case, one[8] expects the cancellation of the two terms of Eq. (4.8) for a coupling resonance $pq < 0$ which yields the weaker detuning, and hence allows a particle to stay in the resonance up to large amplitude, but this is not the case. Besides, since the function F_{pq} which specifies the strength of the resonance $p\bar{\nu}_x - q\bar{\nu}_s = k$ does not depend on the sign of p and q (see Eq. (2.23)), the same argument can be made for the resonance width. One arrives at the conclusion that the functions and the fixed points introduced here are nearly identical for the sum and the difference resonances. In the next section, we study the dynamical motion of particle to estimate the maximum amplitude which will turn out to be almost the same again for the sum and the difference resonances.

V. Dynamics

The Hamiltonian H_c for the resonance $5\bar{\nu}_x + \bar{\nu}_x = 31$ can be plotted as a function of J or I_x as in Fig. 2(a). The higher (lower) curve shows the $\cos(2pq\Psi) = 1$ (-1) case. The top of the higher (lower) curve corresponds to the amplitude $J_s(J_u)$ of the stable (unstable) fixed point. The tunes here are: $\delta_x = -0.0014$, and $\delta_s = 0$. The dot-dash line below the horizontal axis shows the unperturbed part $J\delta_- - C\delta_+$ which is equal to $I_x\delta_x$ for the present parameters. It should be noted that this term is no longer entirely much larger than the perturbation term, on the contrary, it can be smaller than that. This is because our reference system is now rotating with the resonance tune $\bar{\nu}_x$ and $\bar{\nu}_s$, and the rotational energy of a particle is quite small. As going to larger amplitude, the perturbation term gets smaller, reflecting that the beam-beam kick becomes weaker, and the above two solid curves asymptotically merge to the lowest dot-dash line.

Since the Hamiltonian is a constant of motion, a particle moves on the straight line of constant H_c within the range limited by the $\cos(2pq\Psi) = \pm 1$ curves[6,7]. For a fixed initial amplitude J_0, changing the initial phase Ψ_0 means giving a different Hamiltonian. If the initial phase is taken such that the Hamiltonian becomes H_A in Fig. 2, the particle motion can reach the large amplitude beyond the unstable fixed point, while in the case of $H_C = H_B$, the particle trajectory is limited within a narrow region. The physical pictures may be understood by looking at their trajectories in the J,Ψ phase space shown in Fig. 3. As obvious on inspection of the figures, the maximum amplitude J_{max} for a particle with the initial amplitude smaller than J_u is obtained when the initial phase is chosen so that the line of constant Hamiltonian is tangential to the top of the $\cos(2pq\Psi) = -1$ curve as the solid line H_u of Fig. 3. In other words, this is when the initial position of particle is put on the trajectory which passes through the unstable fixed point.

The maximum amplitude J_{max} is common for particles with the amplitude being within J_u and J_{min} which is determined by the left intersection of the constant H_u line and the $\cos(2pq\Psi) = 1$ curve. If the initial amplitude is smaller than J_{min}, the particle motion has no way to be enhanced to reach the large amplitude region, and stays on the trajectory which is somewhat distorted from the unperturbed one. All the points J_u, J_s, J_{max}, and J_{min} depend on the tune δ_x. (In what what follows, we always suppose $\delta_s = 0$).

When $|\delta_x|$ is small, the initial amplitude J_0 is smaller than J_{min}, and enhancement of the trajectory is limited, as shown in Fig. 4(a). At a certain $|\delta_x| = \delta^*_x$, J_0 coincides with J_{min}, and the maximum enhancement is obtained (Fig. 4(b)). As $|\delta_x|$ increases further (Fig. 4(c)), J_{max} becomes smaller and smaller, and is approaching J_0.

The solid line of Fig. 5 shows the calculated maximum amplitude $\hat{X}_{max}$ in the real space versus the tune ν_x for the resonance $5\bar{\nu}_x + \bar{\nu}_s = 31$. It is in excellent agreement with the result of computer simulation[10] which is expressed by the broken line. Both curves show the triangular shape as one can expect from the argument above. The maximum ampli-

tudes $\hat{X}_{max.cal.}$ calculated for some other resonances are tabulated in Table II with the results of simulations $\hat{X}_{max.sim.}$ for comparison . Agreement is quite good. Listed are the tunes which give the maximum value of the maximum amplitudes among other tunes, and those for the calculations agree with those for the simulations.

This good agreement indicates that the single resonance model is quite sufficient for synchro-betatron resonances.

This conclusion validates one advantage of the present Hamiltonian analysis, compared with the computer simulation. Namely, once the functions $F_{oo}(J,C) \pm 2F_{pq}(J,C)$ are calculated, the total Hamiltonian for any tune can be obtained simply adding up the $J\delta_{-} - C\delta_{+}$ term which is just linear in J. Then for a particle with any given initial amplitude, its maximum amplitude can immediately be computed as well as its variation with tune, by changing only the linear term. This may help to save computation time, particularly in the case which requires a very large number of revolutions as for a proton beam.

One thing to be noticed here is that the maximum amplitude for the sum resonance is as big as that for the difference resonance. This is because the Hamiltonian curves as shown in Fig. 2 are similar for both resonances due to F_{pq} which is independent of the sign of p and q. Therefore it is not true that the difference resonance is more dangerous than the sum resonance in the sense that the former can distort the particle trajectory much more than the latter, unless the Hamiltonian curves are so flat that a slight difference of the curves causes a large difference of the maximum amplitude reachable.

VI. Equilibrium particle distribution

So far we have seen that it is possible to have a large enhancement of particle orbits which is, however, not directly linked with particle loss, or emittance blow-up[11]. One might think that since particles, particularly in the tail, can now reach the large amplitude, they may hit the physical aperture, and then be lost, or

the new emittance defined by the new maximum amplitude may be enlarged. However, if all the particles in the tail move to the core as a result of resonance effect, it is possible that there is no particle left on the orbit which can reach the large amplitude, hence neither particle loss, nor emittance blow-up happen. We need to examine the change in the particle distribution.

The equilibrium particle distribution in the presence of the beam-beam effect and the synchrotron radiation effects has been studied by Kheifets[12], Ruggiero[13] and others[14]. They start with the Fokker-Plank equation, and thus the solution can be determined uniquely, independently of the initial distribution. It has not yet been possible to include the synchrotron oscillation into the formalisms.

Here we do not take into account the radiation damping nor the quantum excitation, for simplicity and for spotlighting the pure effect of synchro-betatron resonances. This is a good approximation for a proton beam, and recalling the assumption of a Gaussian distribution for the "strong beam", the system under consideration corresponds to that of an ep storage ring.

In the system which is described by the Hamiltonian, the particle distribution Λ obeys Liouville's theorem:

$$\frac{\partial \Lambda}{\partial \Theta} + \dot{\Psi} \frac{\partial \Lambda}{\partial \Psi} + \dot{J} \frac{\partial \Lambda}{\partial J} + \dot{\Psi}_c \frac{\partial \Lambda}{\partial \Psi_c} + \dot{C} \frac{\partial \Lambda}{\partial C} = 0 \ , \qquad (6.1)$$

where the dot denotes the derivative with respect to Θ. We are interested in the equilibrium distribution achieved after many revolutions, which satisfies

$$\frac{\partial \Lambda}{\partial \Theta} = 0 \ . \qquad (6.2)$$

Since the derivatives satisfy Hamilton's equations, we have

$$[H_c, \Lambda] = 0 \ , \tag{6.3}$$

where the bracket is the Poisson bracket. Classical mechanics says that Λ which satisfies Eq. (6.3) must be a function of the Hamiltonian or constants of motion, i.e.

$$\Lambda = \Lambda(H_c, C) \ . \tag{6.4}$$

We find that Λ is a function only of Ψ, J, and C. The function Λ is normalized such that

$$\int\int\int\int \Lambda \, dJd\Psi dCd\Psi_c = Ne \ , \tag{6.5}$$

where N is the number of particles in a bunch. From the mechanics theory, we can impose no more constraints on Λ.

Let us try other methods. Although ξ is a small number, since the unperturbed term $J\delta_- - c\delta_+$ is not necessarily larger than the perturbation part, we cannot solve Eq. (6.7) in terms of the perturbation method using ξ as an infinitesimally small perturbative parameter. However, if we consider the case where

$$2\xi \frac{\sigma^2}{\beta^*_x} F_{pq}$$

is smaller than the other terms as seen from Fig. 2, we notice that H_c can be divided into two parts according to the order of magnitude as

$$H_c = \underbrace{J\delta_- - C\delta_+ + \xi \frac{\sigma^2}{\beta^*_x} F_{oo}}_{\equiv \ K_0 \ (J.\ C,\ \xi)} + \underbrace{2\ \xi \frac{\sigma^2}{\beta^*_x} \cos(2pq\Psi) F_{pq}}_{K_1 \ (J.\ C,\ \Psi,\ \xi)} \ , \tag{6.6}$$

where

$$K_0 >> K_1 \ . \tag{6.7}$$

The Ψ dependence is only in the K_1 term. The particle distribution function can be Fourier expanded in the J,Ψ phase space because of the periodicity in Ψ with period 2π as

$$\Lambda = \Lambda_0(J,C.\xi) + \sum_{n=1}^{\infty} \cos(2pqn\Psi)\Lambda_{cn}(J,C,\xi)$$

$$+ \sum_{n=1}^{\infty} \sin(2pqn\Psi)\Lambda_{sn}(J,C,\xi) \quad . \qquad (6.8)$$

The Ψ dependence is introduced to Λ only by the K_1 term, so that the ratio $\varepsilon = \left| \frac{\Lambda_{\alpha n}}{\Lambda_0} \right|_{\alpha = c \text{ or } s}$ is of the same order as $\left| \frac{K_1}{K_0} \right|$. With this ε as perturbative parameter, we can develop the perturbation theory. The cost that we pay for this change of perturbative parameter is that $\Lambda_0(J.C,\xi)$ now depends on ξ, and an unknown function differing from the initial distribution. However, $\Lambda_0(J.C,\xi)$ is supposed to be about the initial distribution $\Lambda_0(J.C, \xi = 0)$, for in the laboratory system the nonlinear detuning due to beam-beam effect is small compared with the tune ν_x, so that the particle distribution cannot change much due to such a small perturbation.

For a while we turn our attention to the transverse distribution which is given by the projection of Λ into the transverse phase space:

$$f_x = \iint \Lambda \, d \, I_s d\Psi_s \quad . \quad (6.9)$$

If we perform the integration with respect to Ψ_s, the Ψ dependent parts of Λ drop out, and we find that f_x is a function only of I_x :

$$f_x = f_x \, (I_x) = 2\pi \int \Lambda_0 dI_s \quad . \qquad (6.10)$$

The physical reason for this is that any Ψ_x can produce the same Ψ with a suitable Ψ_s, and hence the Ψ dependence of Λ in the J.Ψ phase space is averaged in the I_x,Ψ_x phase space. After all, it is $\Lambda_0(J,C,\xi)$ which we have to know.

We give up trying to solve $\Lambda_0(J.C,\xi)$ exactly, but we will qualitatively discuss how $\Lambda_0(J,C,\xi)$ "should look" in the presence of a resonance. Substituting Eqs. (4.1), (4,2) and (6.8) into Eq. (6.1), we have

$$2\xi \frac{\sigma^2}{\beta^*_x} \sin(2pq\Psi)F_{pq}[\frac{\partial\Lambda_0}{\partial J} + \sum_{n=1}^{\infty} \frac{\partial\Lambda_{cn}}{\partial J} \cos(2pqn\Psi) + \sum_{n=1}^{\infty} \frac{\partial\Lambda_{sn}}{\partial J} \sin(2pqn\Psi)]$$

$$+ (\delta_- + \nu_{NL}(J.C) + \cos(2pq\Psi)\nu_{pq}) \bullet (- \sum_{n=1}^{\infty} n\,\Lambda_{cn} \sin(2pqn\Psi)$$

$$+ \sum_{n=1}^{\infty} n\,\Lambda_{sn} \cos(2pqn\Psi)) = 0.$$

Multiplying $\sin(2pq\Psi)$, integrating over Ψ, and keeping only the linear term in ε, we obtain

$$\Lambda_1(J,C,\Psi,\xi) = - \frac{2\xi}{\delta_N(J,C,\xi)} \quad \frac{\sigma^2}{\beta^*_x} \; F_{pq} \frac{\partial\Lambda_0}{\partial J} \quad , \tag{6.12}$$

where

$$\delta_N(J,C,\xi) = \delta_- + \nu_{pq}(J,C,\xi) \; . \tag{6.13}$$

The higher harmonic terms Λ_{cn} and Λ_{sn} turn out to be the order of ε^n.

For J much smaller than J_f, the zero of $\delta_N(J,C,\xi)$, which is situated between the unstable and the stable fixed points, δ_N is the same order of ξ (see Eq. (4.3)).

If $(\frac{\partial\Lambda_0}{\partial J})_{\xi = \xi} \sim (\frac{\partial\Lambda_0}{\partial J})_{\xi = 0} \sim O(\frac{1}{I_x} + \frac{1}{I_s})$, Λ_1 is much smaller than Λ_0.

As the amplitude goes close to J_f, the denominator becomes close to zero, and Λ_1 diverges to infinity even if F_{pq} is small. In reality, Λ_1 cannot be bigger than Λ_0, otherwise the number

of particles becomes negative at the phase $\cos(2pq\Psi) = -1$*. It is natural to think that the derivative $\partial\Lambda_0/\partial J$ gets smaller there in order to suppress the divergence:

$$\lim_{J \to J_f} \frac{1}{\delta_N} \frac{\partial \Lambda_0}{\partial J} = \text{const.} \qquad (6.14)$$

For a large value of J_f, the change in the tune with amplitude is slow (this is why the particle motion can reach the large amplitude without detuning of the resonance), with the result that the derivative $\partial\Lambda_0/\partial J$ must be very small in the long range of amplitude.

The change in the equilibrium distribution is sketched in Fig. 6. The flattening effect of Λ_0 prevents the particle density from reducing up to the large amplitude. The size and position of the plateau corresponds to that of the resonance island. When the island is situated in the tail of the distribution like in this example, we can see a blow-up of the tail. In the case that the island is near to the core, the change in the tune with amplitude there is so fast that the plateau may not grow large enough to be observed. This is a plausible explanation of why the observed blow-up of the beam takes place mostly only in the tail in computer simulations[11]. A similar explanation might be valid also for a blow-up of the flat-beam in the tail[15] even in the presence of the radiation damping and the quantum excitation. The flattening of the particle distribution in the resonant particle region can be seen also in plasma physics in the nonlinear effect of Landau damping[16].

VII. Conclusions

We have analysed synchro-betatron resonances due to a crossing angle with the Hamiltonian method, and obtain good numerical agreement with the computer simulations of the particle dynamics. We proved the following:

---

* In an approximation that other terms are neglected.

- The single isolated resonance model is a very good approximation to synchro-betatron resonances.

- The particle motion in the present integrable system with two constants of motion is therefore predictable and analysable. In this sense, the motion is stable.

- Nevertheless, a synchro-betatron resonance can cause a large enhancement of the amplitude of particle trajectories in the transverse phase space. The key of understanding it is that the synchrotron motion which has an energy widely different from the transverse motion, plays a role as energy supply to the transverse motion almost without disturbing itself.

- The resonant island in the tail results in the flattening of the equilibrium particle distribution there. The size of the plateau corresponds to that of the island.

The reason why synchro-betatron resonances are relatively more dangerous than the single resonances due to normal beam-beam interaction without a crossing angle may be as illustrated in Fig. 2; the small curvature, and the widely open area at large amplitude. In the present example, the enhancement factor is 2.5 at most, while the simulation for HERA with a crossing angle shows the factor 6[17]. The situation is possibly as in Fig. 4(a); very flat curves, the most dangerous pattern.

Through many calculations in the present study, the problem of slow convergence of the double summation in the Hamiltonian (2.22) turned out to be no hindrance to the numerical calculation. The total CPU time spent for all the calculations in the present paper was within 20 minutes with CERN IBM 3081. One of the fast calculation methods which can also avoid the false divergence of each term of series due to factorials of large number, etc. is presented in Appendix B.

The particle distribution could not be solved easily, even though the system is described by the simple Hamiltonian for the single resonance, and the synchrotron radiation effects are not included. More elaborate study is necessary for quantitative estimation.

Acknowledgements

The author wishes to thank L.R. Evans for helpful discussions and careful reading of the manuscript. He also would like to thank R. Schmidt for useful suggestions for numerical calculation, and for helpful references, and B. Zotter for helpful suggestions to solve the equilibrium distribution. It is a pleasure to acknowledge the continual encouragement and interest in the present work of J. Gareyte.

Appendix A : Derivation of F_{pq}.

Throughout this appendix, the key of manipulation is to reorder the summation following

$$\sum_{m=0}^{\infty}\sum_{n=0}^{m} b_{mn} = \sum_{n=0}^{\infty}\sum_{m=n}^{\infty} b_{mn} = \sum_{n=0}^{\infty}\sum_{m=0}^{\infty} b_{m+nn} \qquad (A.1)$$

A.1 Applying formula (A.1) to Eq. (2.14) leads to

$$U/(8\pi\xi\ \frac{s2}{\beta^*_x}) = \sum_{n=0}^{\infty} a_n(\alpha_x \cos(W_x+\Psi_x) + \alpha_s \cos\Psi_s)^{2n}$$

$$= \sum_{\ell=0}^{\infty}(\alpha_s \cos\Psi_s)^{2\ell} \sum_{k=\ell}^{\infty} a_k\ {}_{2k}C_{2\ell}\ (\alpha_x \cos(W_x+\Psi_x))^{2(k-\ell)}$$

$$+ \sum_{\ell=1}^{\infty}(\alpha_s \cos\Psi_s)^{2\ell-1} \sum_{k=\ell}^{\infty} a_k\ {}_{2k}C_{2\ell-1}(\alpha_x \cos(W_x+\Psi_x))^{2(k-\ell)+1}$$

$$= \sum_{\ell=0}^{\infty}\sum_{m=0}^{\infty} a_{\ell+m}\ {}_{2(\ell+m)}C_{2\ell}\ (\alpha_s \cos\Psi_s)^{2\ell}(\alpha_x \cos(W_x+\Psi_x))^{2m}$$

$$+ \sum_{\ell=1}^{\infty}\sum_{m=1}^{\infty} a_{\ell+m-1}\ {}_{2(\ell+m-1)}C_{2\ell-1}(\alpha_s \cos\Psi_s)^{2\ell-1}(\alpha_x \cos(W_x+\Psi_x))^{2m-1}$$

(A.2)

A.2 We substitute Eqs. (2.20) and (2.21) into Eq. (A.2) and continue the manipulation. For the first term of Eq. (A.2), this is done below:

$$\sum_{\ell=0}^{\infty}\sum_{m=0}^{\infty} a_{\ell+m}\ {}_{2(\ell+m)}C_{2\ell}(\alpha_x\cos(W_x+\Psi_x))^{2m}(\alpha_s\cos\Psi_s)^{2\ell}$$

$$= \sum_{\ell=1}^{\infty}\sum_{m=1}^{\infty} a_{\ell+m}\ {}_{2(\ell+m)}C_{2\ell}\alpha_x^{2m} \cdot \frac{1}{2^{2m-1}}\left[\sum_{r=0}^{m-1} {}_{2m}C_r \cos 2(m-r)(W_x+\Psi_x) + \frac{{}_{2m}C_m}{2}\right]$$

$$\cdot \frac{1}{2^{2\ell-1}}\left[\sum_{s=0}^{\ell-1} {}_{2\ell}C_s \cos 2(\ell-s)\Psi_s + \frac{{}_{2\ell}C_\ell}{2}\right]$$

$$+ \sum_{m=1}^{\infty} a_m \, {}_{2m}C_0 \, \alpha_x^{2m} \cdot \frac{1}{2^{2m-1}} \left[\sum_{r=0}^{m-1} {}_{2m}C_r \cos 2(m-r)(W_x + \Psi_x) + \frac{{}_{2m}C_m}{2} \right]$$

$$+ \sum_{\ell=1}^{\infty} a_\ell \, {}_{2\ell}C_{2\ell} \, \alpha_s^{2\ell} \cdot \frac{1}{2^{2\ell-1}} \left[\sum_{s=0}^{\ell-1} {}_{2\ell}C_s \cos 2(\ell-s)\Psi_s + \frac{{}_{2\ell}C_\ell}{2} \right]$$

$$= \sum_{\ell=1}^{\infty} \sum_{m=1}^{\infty} a_{\ell+m} \cdot \frac{(2(\ell+m))!}{(2\ell)!\,(2m)!} \, \alpha_x^{2m} \, \alpha_s^{2\ell} \cdot \frac{1}{2^{2(m+\ell)-2}}$$

$$\cdot \left[\sum_{p=1}^{m} \frac{(2m)!}{(m-p)!(m+p)!} \cos 2p\,(W_x + \Psi_x) + \frac{(2m)!}{2(m!)^2} \right]$$

$$\cdot \left[\sum_{q=1}^{\ell} \frac{(2\ell)!}{(\ell-q)!\,(\ell+q)!} \cos 2q\Psi_s + \frac{(2\ell)!}{2(\ell!)^2} \right]$$

$$+ \sum_{m=1}^{\infty} a_m \, \alpha_x^{2m} \cdot \frac{1}{2^{2m-1}} \left[\sum_{p=1}^{m} \frac{(2m)!}{(m-p)!(m+p)!} \cos 2p(W_x + \Psi_x) + \frac{(2m)!}{2(m!)^2} \right]$$

$$+ \sum_{\ell=1}^{\infty} a_\ell \, \alpha_s^{2\ell} \cdot \frac{1}{2^{2\ell-1}} \left[\sum_{q=1}^{\ell} \frac{(2\ell)!}{(\ell-q)!(\ell+q)!} \cos 2q\Psi_s + \frac{(2\ell)!}{2(\ell!)^2} \right]$$

$$= \sum_{p=1}^{\infty} \sum_{q=1}^{\infty} \cos 2p(W_x + \Psi_x) \cos 2q\Psi_s \, \alpha_x^{2p} \, \alpha_s^{2q} \sum_{m=0}^{\infty} \sum_{\ell=0}^{\infty} \frac{(2\,(m+\ell+p+q))!}{m!\,(m+2p)!\,\ell!\,(\ell+2q)!}$$

$$\cdot \frac{a_{\ell+m+p+q}}{2^{2(m+\ell+p+q)-2}} \, \alpha_x^{2m} \, \alpha_s^{2\ell}$$

$$+ \sum_{p=1}^{\infty} \cos 2p(W_x + \Psi_x) \cdot \alpha_x^{2p} \sum_{m=0}^{\infty} \sum_{\ell=1}^{\infty} \frac{(2(\ell+m+p))!}{m!(m+2p)!\,2(\ell!)^2} \cdot \frac{\alpha_x^{2m} \, \alpha_s^{2\ell}}{2^{(\ell+m+p)-2}} \, a_{\ell+m+p}$$

$$+ \sum_{q=1}^{\infty} \cos 2q\Psi_s \, \alpha_s^{2q} \sum_{m=1}^{\infty} \sum_{\ell=0}^{\infty} \frac{(2\,(\ell+m+q))!}{2(m!)^2\,\ell!(\ell+2q)!} \cdot \frac{\alpha_x^{2m} \, \alpha_s^{2\ell}}{2^{(\ell+m+q)-2}} \cdot a_{\ell+m+q}$$

$$+ \sum_{p=1}^{\infty} \cos 2p(W_x + \Psi_x) \cdot \alpha_x^{2p} \sum_{m=0}^{\infty} \frac{(2\,(m+p))!}{m!\,(m+2p)!} \cdot \frac{\alpha_x^{2m}}{2^{(m+p)-1}} \, a_{m+p}$$

$$+ \sum_{q=1}^{\infty} \cos 2q\Psi_s \cdot \alpha_s^{2q} \sum_{\ell=0}^{\infty} \frac{(2(\ell+q))!}{\ell!\,(\ell+2q)!} \, \frac{\alpha_s^{2\ell}}{2^{(\ell+q)-1}} \, a_{\ell+q}$$

$$+ \frac{1}{4} \sum_{\ell=0}^{\infty} \sum_{m=0}^{\infty} a_{\ell+m} \, \frac{(2(\ell+m))!}{(\ell!\,m!)^2} \cdot \frac{\alpha_x^{2m} \, \alpha_s^{2\ell}}{2^{2(\ell+m)-2}}$$

(A.3)

Here, using the formula for product of cosines

$$\cos\theta_1 \cos\theta_2 = \frac{1}{2}\left[\cos(\theta_1 + \theta_2) + \cos(\theta_1 - \theta_2)\right] \qquad (A.4)$$

and defining a new coefficient

$$b_n = \frac{(-1)^{n+1}(2n)!}{n \cdot n!\, 2^{2n-1}} \quad , \quad (n \geq 1)$$
$$= 0 \quad , \quad (n = 0) \qquad (A.5)$$

we can summarize Eq. (A.3) as

$$\text{Eq. (A.3)} = \frac{1}{4} \sum_{m=0}^{\infty} \sum_{\ell=0}^{\infty} b_{\ell+m} \frac{\alpha_x^{2m}\, \alpha_s^{2\ell}}{(m!)^2\,(\ell!)^2}$$

$$+ \frac{1}{4} \sum{}' \cos\left[2p(W_x + \Psi_x) + 2q\Psi_s\right]$$
$$-\infty < p,q < \infty$$

$$\cdot\, \alpha_x^{2|p|}\, \alpha_s^{2|q|} \sum_{m=0}^{\infty} \sum_{\ell=0}^{\infty} b_{\ell+m+|p|+|q|} \frac{\alpha_x^{2m}\, \alpha_s^{2\ell}}{m!\,(m+2|p|)!\;\ell!\,(\ell+2|q|)!}\,, \qquad (A.4)$$

where the prime means that $p + q = 0$ term is excluded from the summation.

A similar manipulation is made for the second term of Eq. (A.2). We obtain

$$\text{The second term} = \frac{1}{4} \sum \cos\left[(2p-1)(W_x + \Psi_x) + (2q-1)\Psi_s\right]$$
$$-\infty < p,q < \infty$$

$$\cdot\, \alpha_x^{|2p-1|} \cdot \alpha_s^{|2q-1|} \sum_{m=0}^{\infty} \sum_{\ell=0}^{\infty} b_{\ell+m+\frac{|2p-1|+|2q-1|}{2}} \frac{\alpha_x^{2m}\, \alpha_s^{2\ell}}{m!\,(m+|2p-1|)!\;\ell!\,(\ell+|2q-1|)!}\,. \qquad (A.5)$$

Combining Eqs. (A.4) and (A.5), and defining the function

$$F_{pq} = \alpha_x^{|p|}\ \alpha_s^{|q|} \sum_{m=0}^{\infty} \sum_{\ell=0}^{\infty} b_{m+\ell+\frac{|p|+|q|}{2}}\ \frac{\alpha_x^{2m}\ \alpha_s^{2\ell}}{m!\ (m+|p|)!\ \ell!(\ell+|q|)!}\ , \tag{A.6}$$

after all we find

$$U = \frac{2\pi\xi\sigma^2}{\beta_x^*}\ [F_{oo}(\alpha_x,\alpha_s) + \sum_{-\infty<p,q<\infty}{}' F_{pq}(\alpha_x,\alpha_s)\ \cos(p(W_x + \Psi_x) + q\Psi_s)]\ . \tag{A.7}$$

Appendix B : A fast numerical calculation method for F_{pq}

First, since the coefficient b_n changed its sign alternatively with n, we should put together the terms of the same sign as follows:

$$F_{pq} = \alpha_x^p \alpha_s^q \sum_{m=0}^{\infty} \sum_{\ell=0}^{\infty} b_{m+\ell+t} \frac{\alpha_x^{2m} \alpha_s^{2\ell}}{m!\,(m+p)!\,\ell!\,(\ell+q)!}$$

$$= \alpha_x^p \alpha_s^q \sum_{n=0}^{\infty} \sum_{\ell=0}^{n} b_{n+t} \frac{\alpha_x^{2(n-\ell)} \alpha_s^{2\ell}}{(n-\ell)!\,(n-\ell+p)!\,\ell!\,(\ell+q)!}$$

$$\equiv \alpha_x^p \alpha_s^q \sum_{n=0}^{\infty} \sum_{\ell=0}^{n} A_{n\ell}$$

$$\equiv \alpha_x^p \alpha_s^q \sum_{n=0}^{\infty} B_n \quad , \tag{B.1}$$

where $t = \frac{p+q}{2}$. (B.2)

The series B_n now changes the sign alternatively. The convergence judgement condition of series may be, for instance,

$$\left| \frac{B_n}{\sum_{\ell=0}^{n-1} B_\ell} \right| < \varepsilon \quad , \tag{B.3}$$

where ε is a certain small number.

If we directly calculate $A_{n\ell}$ from the definition as it is, the factorials or the powers of α_x and α_s may cause the false numerical overflow. Namely, although the ratio does not diverge, the numerator or the denominator is overflowed in the middle of individual calculation. Meanwhile, looking at Eq. (B.1) carefully, we find the following recurrence equation for $A_{n\ell}$:

$$A_{n\ell} = \frac{A_{n-1\ell}\ \alpha_x^{\,2}}{(n-\ell)(n-\ell+p)}\ r_n \qquad (\ell \leq n-1) \qquad (B.4)$$

$$A_{nn} = \frac{\alpha_s^2}{n\ (\ n+q)}\ r_n \qquad (B.5)$$

with

$$A_{oo} = \frac{b_t}{p!q!} \qquad (B.6)$$

where

$$r_n = \frac{b_{n+t}}{b_{n+t-1}} = -\frac{(2(n+t)-1)\ (n+t-1)}{2(n+t)} \qquad (B.7)$$

Of the functions above, only r_n increases with n, but the increase is just linear in n. Calculating $A_{n\ell}$ in order avoids not only the false overflow but also repetition of calculation of the same factorial, which greatly reduces the computation time.

References

1) A. Piwinski, Proc. 11th Intern. Conf. on High-Energy Accelerators, CERN (Birkhäuser Verlag, Basel, 1980) p. 638.

2) A. Piwinski, DESY 77/18, 1977.

3) A. Piwinski, DESY 78/8, 1978.

4) T. Suzuki, Part. Accelerators, 12, 237 (1982).

5) E.D. Courant, R.D. Ruth and W.T. Weng, (AIP Conf. Proc. No. 127, 1983), p. 294.

6) P. Bambade, thesis, University de Paris-Sud, LAL, 84/21, 1984.

7) L.R. Evans, CERN SPS/83-38 (DI-MST), 1983.

8) P. Bambade, LAL/RT/84-2, 1984.

9) B.W. Montague, Nucl. Instrum. Methods, 187, 335 (1981).

10) The equations of motion for simulations are given in Ref. 3.

11) A. Piwinski, private communication.

12) S. Kheifets, Part. Accelerators, 15, 153 (1984).

13) F. Ruggiero, Ann. Phys. (N.Y.) 153, 122 (1984).

14) J.F. Schonfeld, Fermilab-Conf-85/18-T, 1985.

15) H. Wiedemann, (AIP Conf. Proc. No. 57, 1979), p.84.

16) N.A. Krall and A.W. Trivelpiece, Principle of Plasma Physics (McGraw-Hill, New York, 1973), p.512.

17) A. Piwinski, CERN LEP-TH/85-10, 1985.

Table I

Parameters for the DORIS[3)]

E_o	: beam energy (GeV)	1.8
ξ	: beam - beam parameter	0.01
β^*_x	: beta-function at the collision point (m)	1
σ	: effective transverse beam size (mm)	0.23
ν_s	: synchrotron tune	0.034
h	: harmonic number	480
α	: momentum compaction factor	0.018
C	: circumference (m)	288
$\hat{x}_{ini}$	: initial transverse amplitude (mm)	0.8
$(\hat{\Delta E/E_o})_{ini}$	: initial synchrotron amplitude	1.8×10^{-3}
a	: half of the crossing angle (mrad)	12

Table II

The maximum amplitude for some resonances

($\hat{X}_{ini}$ = 0.8 mm, $\nu_s = \bar{\nu}_s$ = 0.034)

resonance	$\bar{\nu}_x$	ν_x	$\hat{X}_{max.cal.(mm)}$	$X_{max.sim.(mm)}$	$\frac{\hat{X}_{max.cal.}}{\hat{X}_{max.sim.}}$
$5\bar{\nu}_x + \bar{\nu}_s = 31$	6.1934	6.19208	1.902	1.887	1.008
$5\bar{\nu}_x - \bar{\nu}_s = 31$	6.2068	6.2057	1.923	1.892	1.016
$4\bar{\nu}_x + 2\bar{\nu}_s = 25$	6.233	6.2320	1.862	1.909	0.975
$4\bar{\nu}_x - 2\bar{\nu}_s = 25$	6.267	6.2660	1.855	1.831	1.013
$5\bar{\nu}_x + \bar{\nu}_s = 32$	6.3932	6.3921	1,923	2.026	0.949
$5\bar{\nu}_x - \bar{\nu}_s = 32$	6.4068	6.4057	1.923	1.872	1.027
$7\bar{\nu}_x + 3\bar{\nu}_s = 45$	6.414	6.4124	1.206	1.337	0.902
$7\bar{\nu}_x - 3\bar{\nu}_s = 45$	6.4431	6.44155	1.209	1.193	1.013

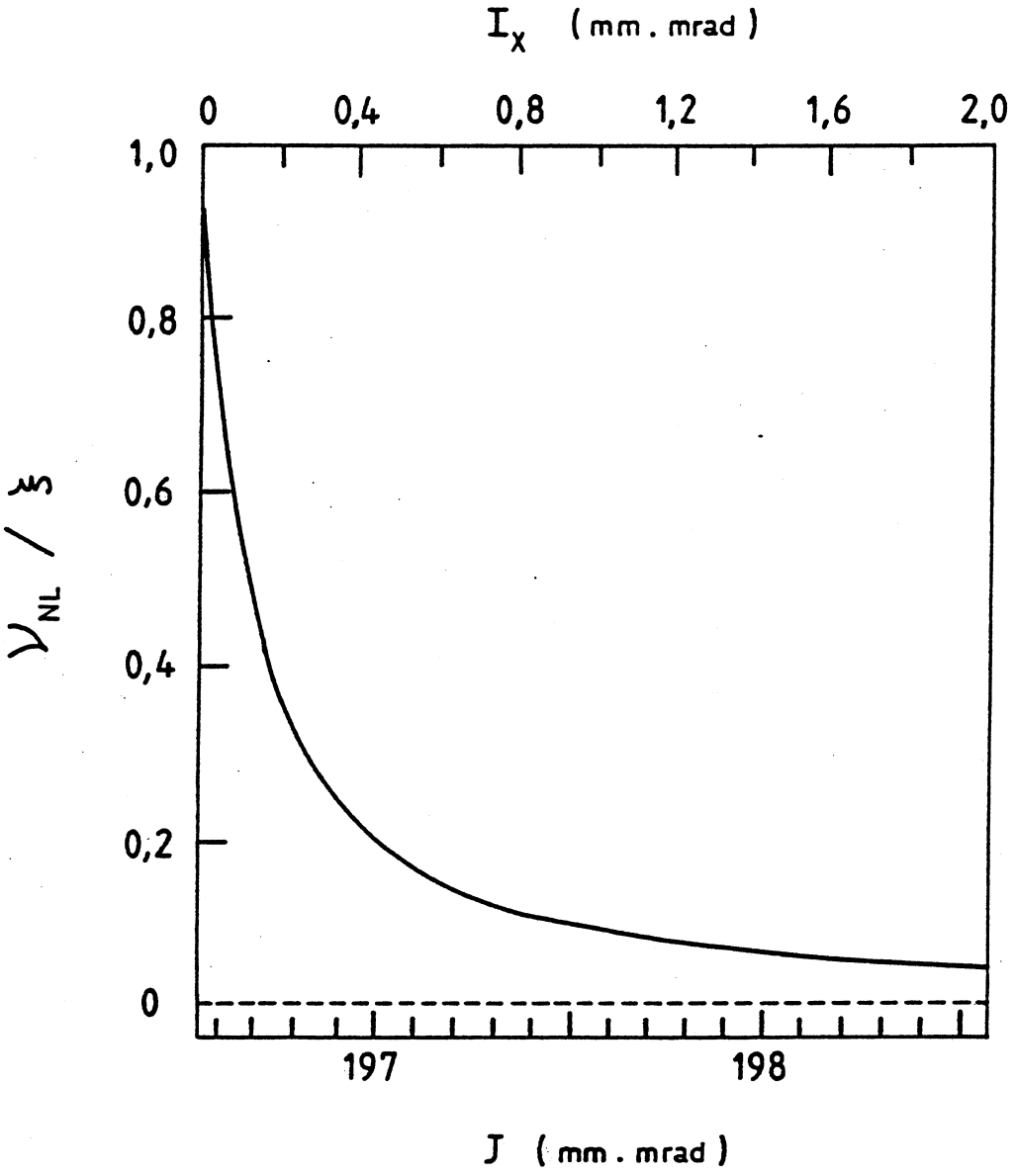

Fig. 1 Detuning curve.
The scale of J is for the resonance $5\bar{\nu}_x + \bar{\nu}_s = 31$.

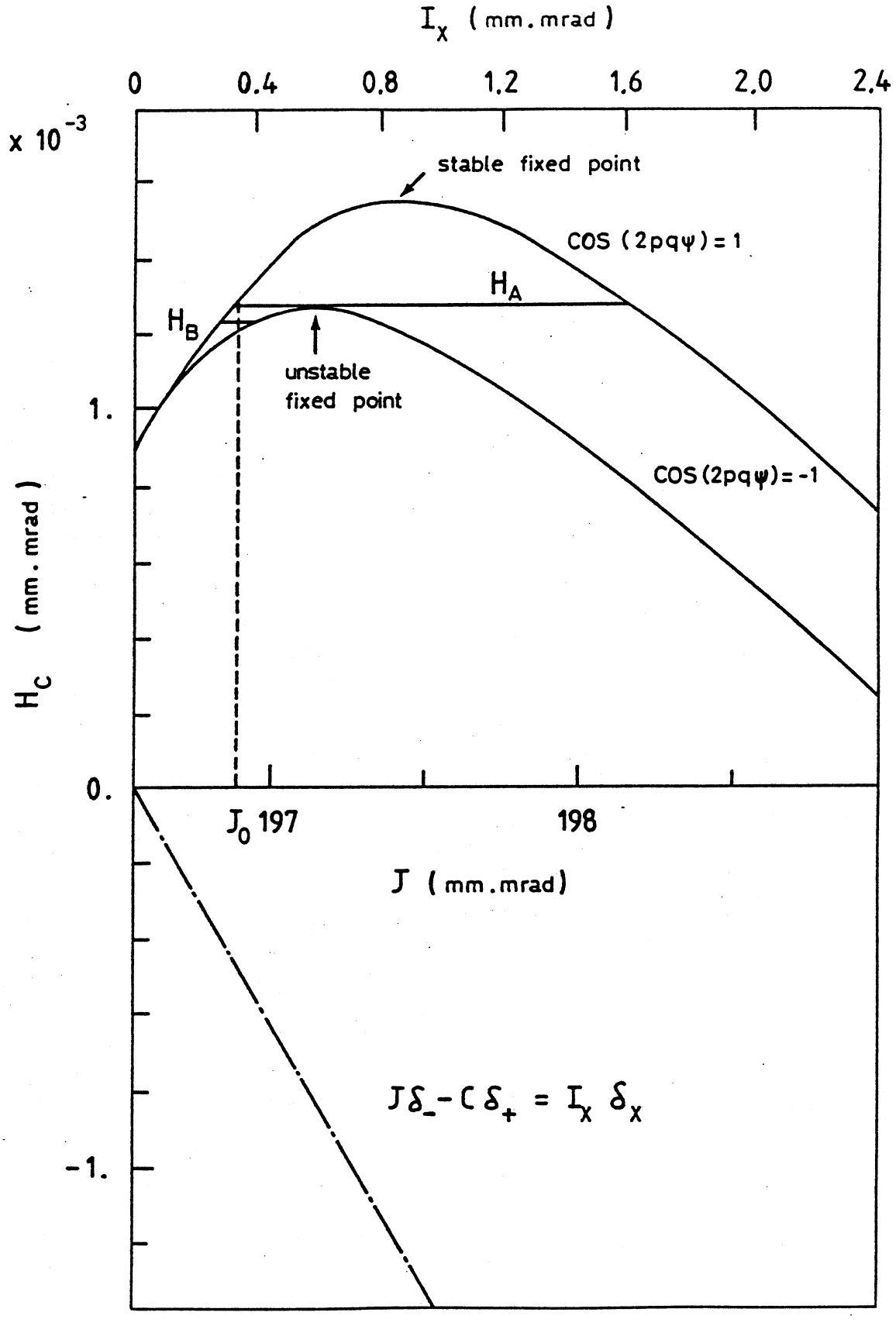

Fig. 2 The Hamiltonian H_C for the resonance $5\bar{\nu}_x + \bar{\nu}_s = 31$. ($\delta_x = -0.0014$, $\delta_s = 0$).

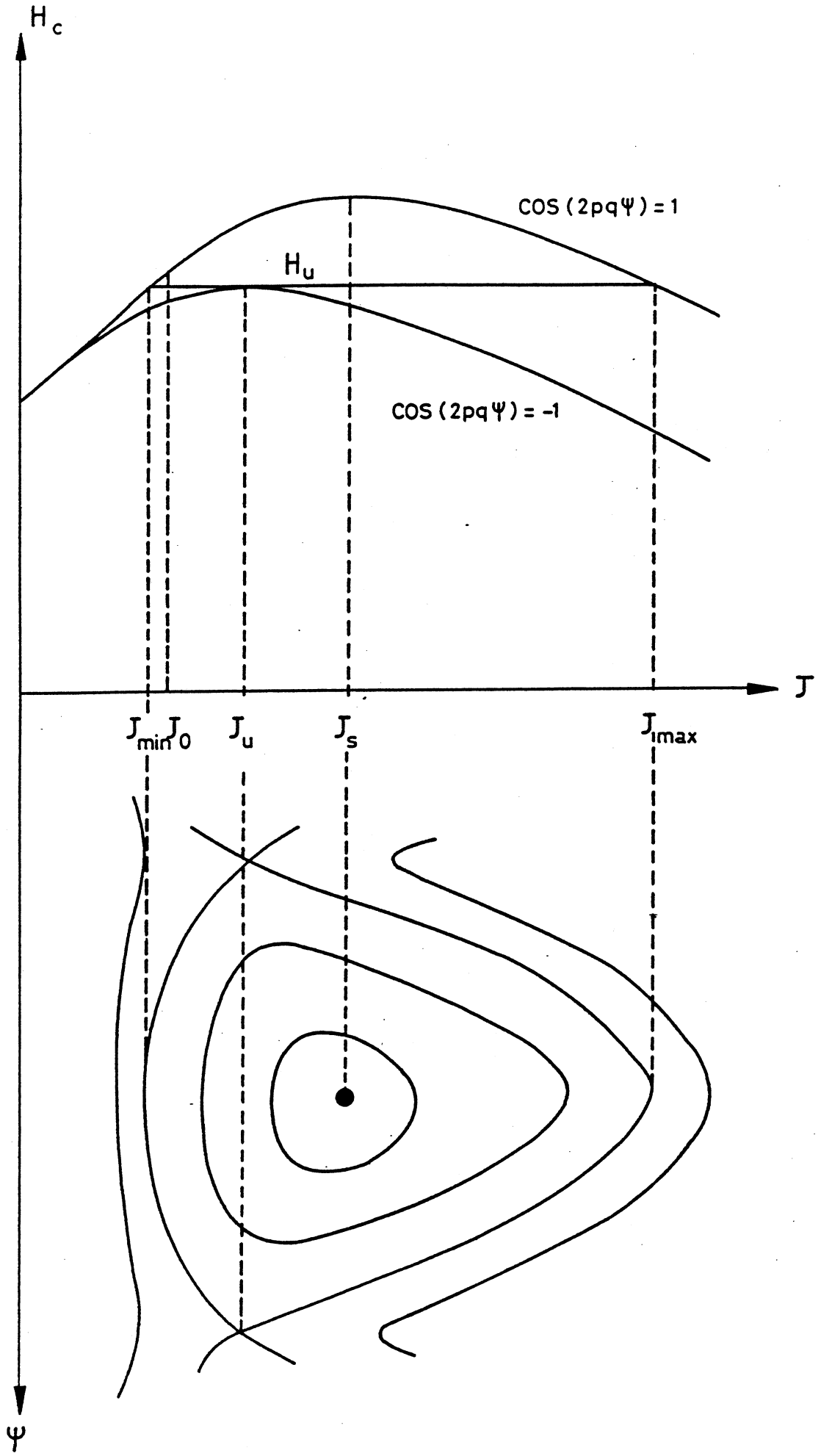

Fig. 3 Particle trajectory in the J,ψ phase space.

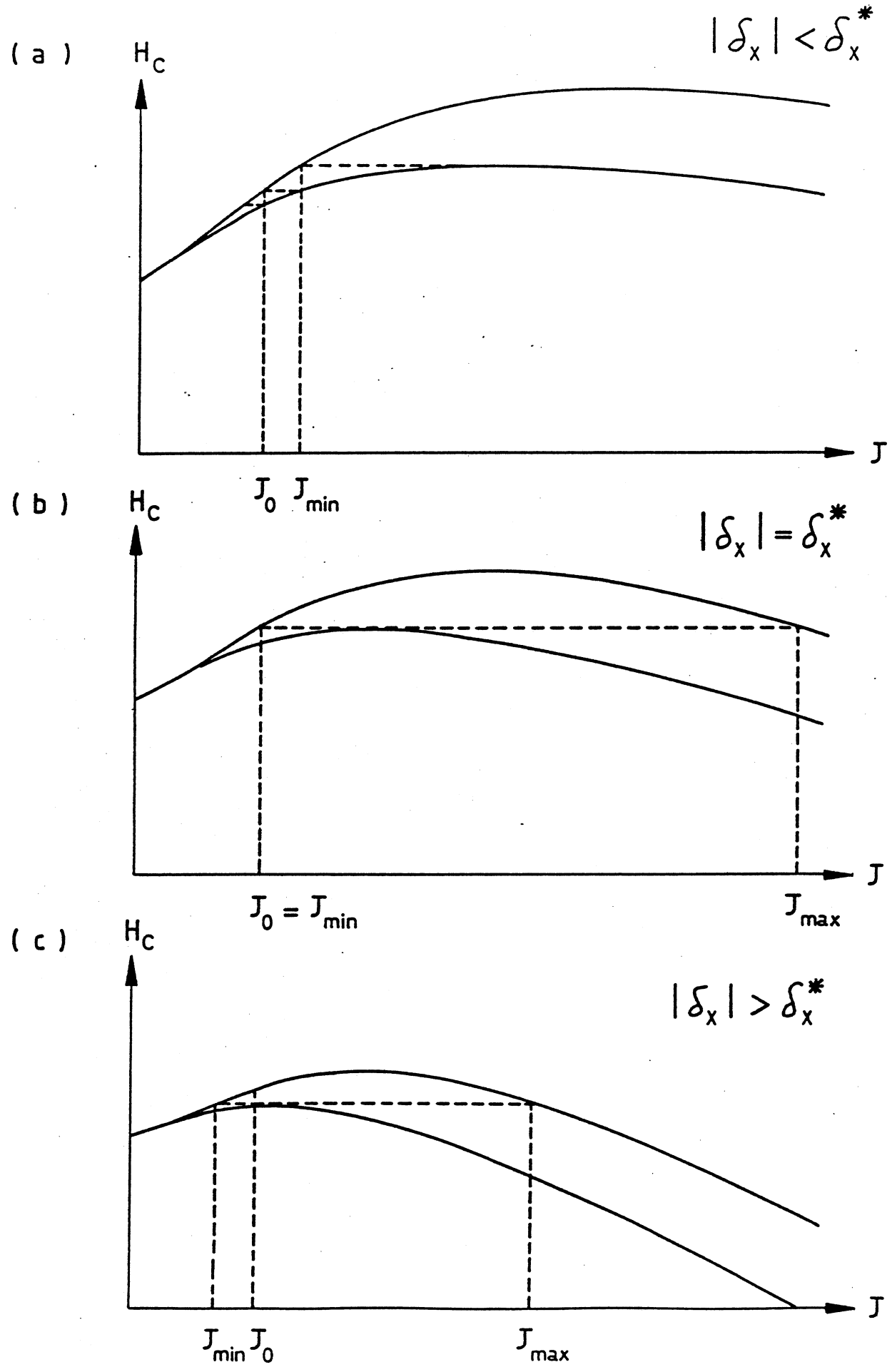

Fig. 4 Change of J_{max} with δ_x .

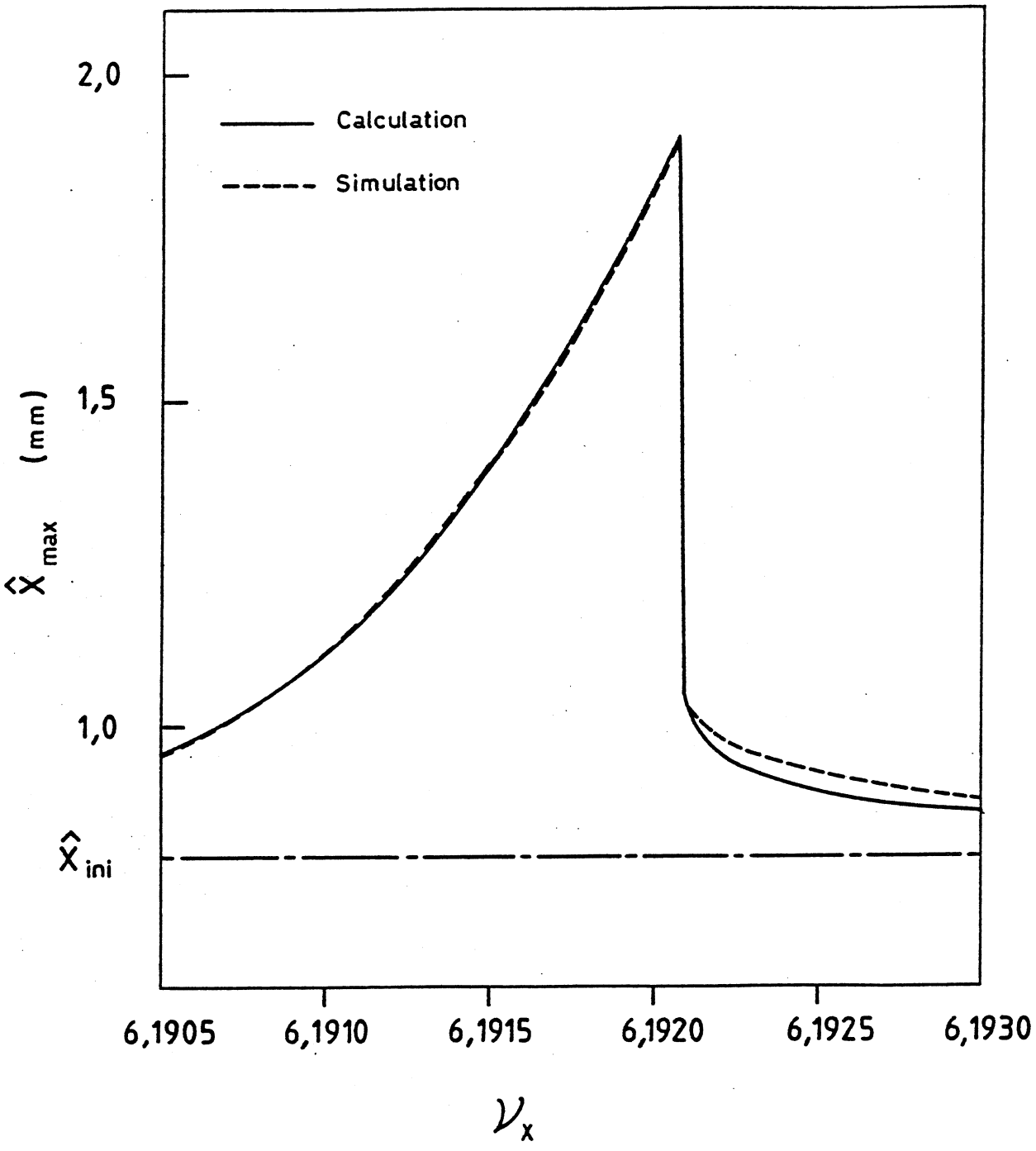

Fig. 5 The maximum amplitude $\hat{X}_{max}$ in the real space versus ν_x for the resonance $5\bar{\nu}_x + \bar{\nu}_s = 31$.

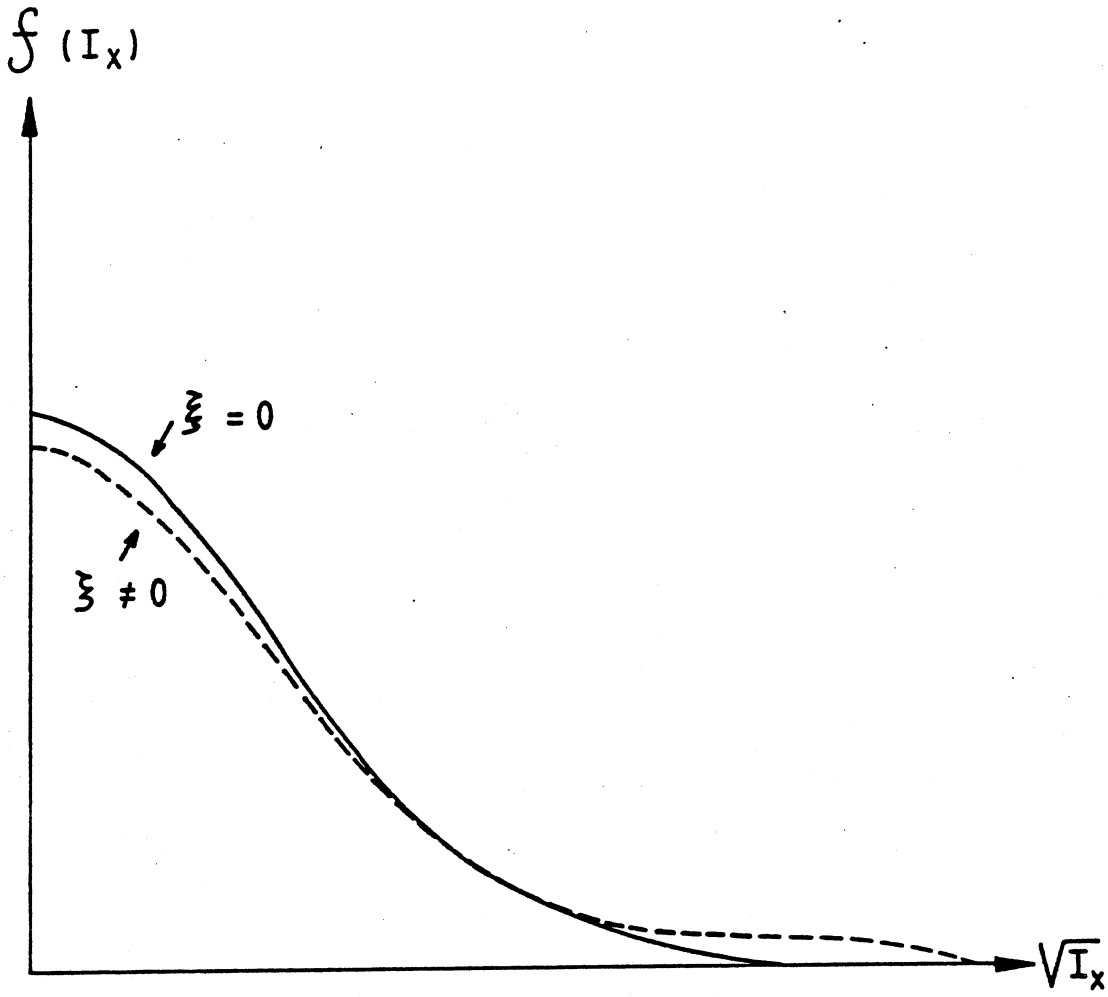

Fig. 6 Sketch of the change in the equilibrium particle distribution. The flattening occurs around the resonance island.